Clinical Characterization of Aerosolized *Francisella tularensis* Infection in Cynomolgus macaques

Ondraya M. Frick[1], Virginia A. Livingston[1], Chris A. Whitehouse[2@], Rebecca A. Erwin-Cohen[1], Aimee I. Porter[1], Derron A.Alves[3&], Aysegul Nalca[1*]

[1]Center for Aerobiological Sciences, [2]Molecular Toxicology Division, [3]Pathology Division U.S. Army Medical Research Institute of Infectious Diseases (USAMRIID), Fort Detrick, Maryland

*Corresponding author. Address: Center for Aerobiological Sciences, U.S. Army Medical Research Institute of Infectious Diseases, 1425 Porter Street, Frederick, MD 21702, United States. Tel: +1 301-619-8495; E-mail address: aysegul.nalca.civ@mail.mil

Current Address:
[@] Division of Animal and Food Microbiology, Center for Veterinary Medicine, Food and Drug Administration
[&] Veterinary Pathology Services, Joint Pathology Center, Silver Spring, MD

Running Head: *Aerosolized Francisella tularensis*

Keywords: *Francisella tularensis*, tularemia, aerosol, animal model

Disclaimer: Opinions, interpretations, conclusions, and recommendations are those of the authors and are not necessarily endorsed by the US Army or the Department of Defense.

Abstract

The disease progression and pathogenesis of tularemia was examined in three species of NHPs (African green monkey (AGM), cynomolgus macaque (CM), rhesus macaque (RM)) exposed to aerosolized *Francisella tularensis* in a previous study. Based on the similarity of infectious dose, clinical symptoms and disease progression with human tularemia, the CM was the most appropriate animal species to develop an animal model to test potential medical countermeasures against inhalational tularemia. In this study, the disease pathogenesis of inhalational tularemia was investigated after exposing cynomolgus macaques to target doses of 50, 500 or 5000 CFU of aerosolized F. tularensis SCHU S4. Survival was challenge dose dependent with target doses of 500 CFU (range of 134 to 749 CFU) and 5000 CFU (range of 1177 CFU to 5860 CFU) causing 100% lethality by Days 17 and 8 respectively. Target doses of 50 CFU (range of 10 CFU to 110 CFU) resulted in 20% survival. Comparable to respiratory tularemia infection in humans, infection of cynomolgus macaques with aerosolized SCHU S4 resulted in fever, anorexia, increased white blood cell (WBC) counts, increased liver enzymes, and pathology typical of infection with F. tularensis regardless of the challenge dose. These results indicated that *F. tularensis*-infected cynomolgus monkeys have similar clinical profiles as seen in humans and are reliable animal models to test medical countermeasures against aerosolized *F. tularensis.*

Introduction

Francisella tularensis causes an acute febrile illness called tularemia in humans. However, the disease can manifest as a range of possible clinical presentations, largely depending on the route of infection, dose, virulence of the bacterial strain, and host immune response [1]. After exposure, *F. tularensis* multiplies at the initial site of infection prior to spreading to the regional lymph nodes, liver, and spleen [2]. The most common form of disease is the ulceroglandular, involving an ulcer at the inoculation site and regional lymphadenopathy, which is commonly acquired by direct contact with infected animals or arthropod bites [3]. Less commonly, variations of ulceroglandular disease are associated with different inoculation sites and include oculoglandular and oropharyngeal disease. The oropharyngeal form results from ingesting contaminated food or water and, while rare, it has been reported with increasing frequency in Turkey and other European countries [4-6]. Pulmonary disease (pneumonic tularemia) can result from clinical progression of the ulceroglandular forms or can occur from direct inhalation of *F. tularensis* organisms. Pneumonic tularemia has a 30-60% case-fatality rate if left untreated, which can be reduced to 3% if treated early with antibiotics [7]. Small particles of aerosolized *F. tularensis* can travel through the upper respiratory tract and into the alveoli when inhaled. Here alveolar clearance is normally achieved by phagocytic cells (e.g., alveolar macrophages or polymorphonuclear leukocytes), which normally engulf invading bacteria and clear them from the lungs. Further clinical progression from any of the forms of tularemia can result in septic tularemia leading to a state of septic shock [3]. *F. tularensis* is highly successful at causing a systemic infection because of its ability to evade the immune system, principally by evading phagocytosis and replicating within macrophages, which plays a role in dissemination of the infection to distant sites within the body (via trafficking through the regional lymph nodes into the bloodstream) [8].

The high lethality of type A *F. tularensis*, its extreme respiratory infectivity, and high survivability as an aerosol has led to its inclusion in the list of potential biological weapons. Historically, *F. tularensis* has been studied by Japan and the former Soviet Union for its potential as a biological weapon, and it was included in the United States offensive biological weapons program until that program was discontinued in 1969 [2, 9, 10]. Furthermore, for these reasons, the organism is currently listed as a Category A threat agent by the Centers for Disease Control

and Prevention (CDC) [2, 11]. The intentional release of aerosolized *F. tularensis* in a densely populated area could cause a large number of cases in only a few days [12]. Furthermore, naturally occurring outbreaks of pneumonic tularemia still occur in the United States, as exemplified by outbreaks in Martha's Vineyard, Massachusetts in the summer 1978 and again in 2000 [13, 14].

Models of tularemia disease have been evaluated in a variety of animal species including mice, rabbits, rats, guinea pigs and monkeys [15]. In a previous study, we compared the LD_{50} and disease outcome of inhalational tularemia in three NHP species (cynomolgus and rhesus macaques and African green monkeys) [16]. Based on these data, the cynomolgus macaque appears to be the species that most closely mirrors human disease resulting from inhalation exposure to *F. tularensis*. Thus to more extensively characterize the disease progression and pathogenesis in this model, in this study, we exposed groups of cynomolgus macaques to three different target doses (50 CFU, 500 CFU, and 5000 CFU) of aerosolized *F. tularensis* SCHU S4. The resulting data from this study will be critical knowledge needed for using this model for evaluation of vaccines and therapeutics for tularemia to satisfy the FDA *Animal Rule*.

Materials and Methods

Animals and Ethical Statement

Twenty eight healthy, adult cynomolgus macaques (*Macaca fascicularis*) of both sexes weighing >4.0kg were obtained from the United States Army Medical Research Institute of Infectious Diseases (USAMRIID) nonhuman primate (NHP) colony. All animals exposed to *Francisella tularensi*s were handled in a BSL-3 containment laboratory at USAMRIID. Research was conducted in compliance with the Animal Welfare Act and other federal statutes and regulations relating to animals and experiments involving animals, and adhered principles stated in the Guide for the Care and Use of Laboratory Animals, National Research Council, 2011. The facility where this research was conducted (USAMRIID) is fully accredited by the Association for the Assessment and Accreditation of Laboratory Animal Care International. Research was conducted under a protocol approved by the Institutional Animal Care and Use Committee (IACUC) at USAMRIID. All animals were examined and evaluated twice per day by study personnel. Early endpoint criteria, as specified by the score parameters within the

"Post-exposure observations" section of these methods, were used to determine when animals should be humanely euthanized.

Bacteria

Francisella tularensis SCHU S4 strain was provided by the National Institute of Allergy and Infectious Diseases. A 25-ml flask of Mueller Hinton II (MHII) liquid medium containing 2% IsoVitaleX was inoculated with 10 µL of a SCHU S4 seed stock. After 23 hours of incubation at 37°C and shaking at 200 rpm, the optical density (OD_{660} nm) was measured and the bacteria were diluted to the desired nebulizer concentration in MHII medium.

Aerosol exposures

Each macaque was anesthetized by intramuscular (i.m.) injection of tiletamine/zolazpam (3 mg/kg) and challenged by aerosol as previously described [17]. Briefly, the respiratory function of each of the NHPs was measured using whole-body plethysmography (Buxco Systems, Sharon, CT) before aerosol challenge. Aerosol procedures were conducted using a 16-liter, airtight Lexan chamber assembled in a head-only configuration for individual NHP exposures in a class III biological safety cabinet located inside a BSL-3 suite. All airflows, environmental monitoring, and system balancing were configured, controlled, and recorded through the institute standard automated bioaerosol exposure system (ABES). Integrated air samples were obtained for each individual exposure using an all-glass impinge (AGI) drawing from a port centered on the chamber and opposite to the animal's head. Small-particle aerosols were generated with a three-jet Collison nebulizer running at 7.5 liter/min.

Telemetry

Macaques were implanted subcutaneously with a radiotelemetry device (Data Sciences International DSI), St. Paul, MN) at least 14 days before aerosol exposure. Body temperatures were recorded every 15 minute by the DataQuest A.R.T. 4.1 system (DSI). Pre-exposure data were used as a baseline to fit an autoregressive integrated moving average (ARIMA) model. Temperature elevations exceeding three standard deviations over the baseline were used to compute fever duration, hours, and average elevation. Fever was defined as elevation of body temperature $\geq 1.5^{o}$C over baseline values for each individual animal. Baselines for each animal

were calculated by averaging the recorded 15 minute temperature intervals for three days prior to challenge. Due to telemetry equipment failure, two animals in the high target dose group had shorter baselines starting Day -1.5 and Day -0.5; for these animals, temperature recordings were initiated around 12:00 PM on respective days.

Post-exposure observations

Macaques were observed at least twice a day after aerosol exposure. Macaques were scored for clinical signs of disease prior to, and while under anesthesia. The scoring parameters were: responsiveness and appearance (0: active; 2: depression, mild unresponsiveness; 3: head down, hunched; 4: moderate unresponsiveness; 5: severe unresponsiveness), dyspnea (0: normal breathing; 2: mildly labored; 3: labored; 5: agonal breathing), dehydration (0: not present; 1: mild; 2: moderate; 3: severe), anorexia (0: eating; 1: no biscuits for 1 day but eats enrichment; 2: no biscuits for 2 days or not eating enrichment), rash (0: none; 1: slight; 2: moderate; 3: severe), cough (0: none; 1:≤2 coughs/5 min; 2: 3–10 coughs/5 min; 3: ≥10 coughs/5 min), nasal discharge (0: none; 1: mild; 2: moderate; 3: severe), urine (0: normal; 3: none), stool (0: normal; 1: loose stool, 2: liquid stool or none), and fever (0: no change, 1: baseline +1°C; 2: baseline +2°C or higher; 3: baseline – 2°C). Macaques were also evaluated for changes in weight (0: no change; 1: baseline-10–15%; 2: baseline – 15%; 3: baseline – 20%) and the presence of lymphadenopathy (0: <3 mm; 1: 3–9 mm; 2: >10–19 mm; 3: >20 mm). The early endpoint criteria for humane euthanasia, indicative of very poor health status, were cumulative clinical scores of 15–20 (maximum score), and/or a sudden drop of >3°C from baseline body temperature.

Clinical laboratory evaluation

Blood samples were collected from central venous catheters (CVC) inserted in the internal jugular vein beginning fourteen days before, one day before, days 1 - 21 and day 28 after exposure. If collection from the CVC was not possible, blood samples were collected from the femoral vein of macaques anesthetized with 3 mg/kg i.m. tiletamine/zolazepam. Samples collected one day prior to exposure served as a normal reference baseline for each animal. CBCs and blood chemistries were analyzed with Beckman Coulter hematology and VITROS 250 chemistry analyzers, respectively.

DNA extraction and real time quantitative real-time PCR assay (qRT-PCR)

DNA from blood and tissue samples was extracted using a DNeasy Blood and Tissue Kit (Qiagen, Valencia, CA) according to the manufacturer's instructions. Quantitative real-time PCR was performed with the LightCycler (Roche, Indianapolis, IN) using a *Francisella tularensis* (*tul4*) assay as previously described [18].

Necropsy

A full necropsy was performed under direct supervision of a pathologist board certified by the American College of Veterinary Pathologist in a biosafety level (BSL) 3 necropsy facility. Tissues samples from all major organ systems (respiratory, gastrointestinal, genitourinary, lymphoid, neurologic, endocrine, skin and mucous membranes) were collected from each animal for bacterial counts and histopathological and immunohistochemical examination. Tissue samples for bacterial count determination were frozen at -70°C until processed. All other tissues were immersion-fixed in 10% neutral buffered formalin for a minimum of 21 days prior to removal from biocontainment.

Histology and immunohistochemistry

Formalin-fixed tissues for histologic examination were trimmed, processed, and embedded in paraffin according to established protocols [19]. Histology sections were cut at 5-6 µm on a rotary microtome, mounted on glass slides, and stained with hematoxylin and eosin (H&E). Tissues evaluated by immunohistochemistry were stained for *F. tularensis* lipopolysaccharide (LPS) (Meridian Life Science, Inc, Cincinnati, OH) using a mouse monoclonal antibody (USAMRIID immuno #927) and an immunoperoxidase assay system (EnVision System, DAKO Corp., Carpinteria, CA). Unstained tissue sections were deparaffinized, rehydrated, subjected to methanol-hydrogen peroxide block, rinsed, and pretreated with proteinase K for 6 minutes at room temperature. A serum-free protein block (DAKO) plus 5% normal goat serum was applied for 30 minutes. The monoclonal antibody was then applied to the tissue at a dilution of 1:1200 and incubated at room temperature for 60 minutes. The tissue was exposed to the EnVision horseradish peroxidase labeled polymer for 30

minutes at room temperature. All sections were exposed to 3,3'-diaminobenzidine (DAB) permanent chromogen for 5±1 minutes, rinsed, counter-stained with hematoxylin, dehydrated, and cover-slipped with Permount. Normal uninfected lung tissue served as the negative control; the positive control tissue was lung tissue from a known *F. tularensis*-infected monkey. Normal mouse IgG was used as the negative serum control for the control slides.

Statistical analysis

NHP body temperatures were recorded by telemetry. Pre-exposure temperature data taken between 12 hours and three days pre-exposure was used to develop a baseline period to fit an autoregressive integrated moving average (ARIMA) model. Forecasted values for the post exposure periods were based on the baseline extrapolated forward in time using SAS ETS (vers. 9.3). For body temperature, residual changes greater than two standard deviations were used to compute fever duration (number of hours of significant temperature elevation), fever hours (sum of the significant temperature elevations), and average fever elevation (fever hours divided by fever duration in hours). The number of surviving animals in each group was statistically insufficient at later time points; therefore only post-exposure data through Day 8 was used for analysis. T-tests with stepdown bootstrap adjustment were utilized to compare mean temperature variables between groups. ANOVA at each individual time point was completed with post-hoc Tukey's tests for pair-wise comparisons for CBCs and chemistries for time points Day 0 through Day 8. Beyond time point Day 8, there were insufficient samples for comparison. Kruskal-Wallis and Wilcoxon-Mann-Whitney (pairwise comparison) tests were used for analysis of bacterial load in blood samples among groups at individual time points and test of bacterial load from tissue samples among groups. Results were significant at $P<0.05$.

Results

Survival and clinical signs

Three groups of cynomolgus macaques were exposed to increasing doses of aerosolized *F. tularensis* (Table 1). The target doses were 50 CFU (n=10), 500 CFU (n=9) and 5000 CFU (n=9) and were chosen based on lethal dose$_{50}$ (LD_{50}) optimization we previously determined

[16]. The calculated inhaled doses were comparable to the target doses for each group (Table 1). Survival was dose dependent, with the high target dose group receiving 5000 CFU (range of 1,177 CFU to 5,860 CFU) and the intermediate target dose group receiving 500 CFU (range of 134 to 749 CFU), both resulted in 0% survival. The low target dose group received 50 CFU (range of 10 CFU to 110 CFU) which resulted in 20% survival (Figure 1). There were significant differences in the survival curves when comparing the low dose group to the intermediate (P=0.0324) and high dose groups (P=0.0036) (Table 2). Except one animal in the intermediate dose group, the majority of macaques receiving 5000 CFU dose and 500 CFU met criteria for euthanasia between days 6 – 8; whereas, animals receiving 50 CFU dose had a much wider range, meeting criteria for euthanasia between 7 – 19 days (Table 1).

The onset of fever was dose dependent. The high, intermediate, and low target dose groups showed significant increases in temperature beginning on days 2.8, 3.5, and 4.2, respectively (Figure 2). There was no significant difference between groups for fever duration or average elevation. Decreased appetite and activity were also observed by day 3. Over half of the animals developed a cough and 78% of the high dose group developed a cough between days 7 – 9. Loose stool was observed in 25% animals, primarily in the low dose group. Body weights of all animals were taken on day -1 and on the day of euthanasia. The high and intermediate dose groups showed similar weight loss of 8.3% (P=0.0171) and 8.7% (P=0.0171), respectively; whereas, the low dose group lost an average of 2.4% (Table 1).

Clinical laboratory evaluation

Changes in CBCs and blood chemistries were observed in all groups after exposed to *F. tularensis*. White blood cell (WBC) counts increased starting day 2 for the high and low dose group and day 3 for the intermediate dose group (Figure 3A). Values peaked within 48 hours after initial increase for both the high and intermediate dose groups and within 96 hours for the low dose group. All groups showed increases in neutrophils (NEU) over time (P<0.0001) that exceeded the normal range by day 4, although only the low and intermediate dose groups increases above the normal range were statistically significant (P<0.05) (Figure 3B). In contrast, lymphocytes (LYM) showed a sharp decrease starting on day 2 for all groups (Figure 3C). Platelets (PLT) dropped steadily starting on day 2 for all groups, although they did not fall

outside of the normal range (Figure 3D). There were group-wise differences noted for the low versus high and intermediate versus high dose groups for WBC (P=0.0110, P=0.0437), LYM (P<0.0001, P=0.0012), and PLT (P=0.0250, P=0.0174), respectively.

Evaluation of serum chemistries showed changes in total protein, albumin, lactate dehydrogenase (LDH), aspartate and alanine transaminases (AST and ALT), and alkaline phosphatase (ALKP) (Figures 4A - F). Total protein and albumin values decreased in all three groups by day 3, although there were no significant differences in total protein between the three groups (Figure 3A). In contrast, albumin values were significantly lower in the intermediate (p=0.0003) and high dose groups (0.0014) compared to the low dose group (Figure 4B). In addition, both intermediate and high dose group values were significantly lower than the normal range (<0.05). Liver enzymes AST, ALT and ALKP were elevated in all groups (Figure 4C-E). Pair-wise comparisons showed significant differences between the low and high dose groups for AST, ALT, and ALKP (P=0.0062, P=0.0118, and P<0.0001, respectively). The greatest increases outside of the normal range were observed in elevated ALKP values for the high dose group on days 6 (P<0.001), 7 (P<0.01) and 8 (P<0.001). Levels of LDH increased starting on day 4 for all groups with the high dose group showing the greatest increases in comparison to the low dose group (P=0.0385) (Figure 4F).

Blood and tissue bacterial load

Whole blood samples were collected from exposed animals for bacterial load using real-time PCR (Figure 5). In the blood, bacterial genomes were detected as early as day 5 for the intermediate and high dose groups and day 6 for the low dose group. Bacterial load peaked day 8 for both intermediate and high dose groups (Figure 5A).

DNA was extracted for real-time PCR from selected tissues of animals euthanized during the study due to severe disease. Bacterial genomes were detected in all tissues examined for every dose group (Figure 5B). As expected, lung and tracheobronchial lymph node had the highest bacterial loads reaching 10^7 genomes/g in the low dose group and 10^9 and 10^8 genomes/g in the intermediate and high dose groups, respectively. Spleen and bone marrow also had high bacterial loads reaching 10^8 genomes/g in all exposure groups and the high dose group, respectively (Figure 5B). Generally the high dose group had higher levels of genomes/g in the

tissues tested compared to the other two groups with the exception of the kidney, tracheobronchial lymph node, and adrenal gland. The two surviving animals had undetectable levels of bacterial genomes in all tissues tested (data not shown).

Pathology

Gross and histopathologic features of animals euthanized during the study were examined. The gross postmortem lesions observed in this study were similar to those previously reported regardless of the dose received, and/or the time-to-death following *F. tularensis* exposure [16]. The most notable lesions were observed in the thoracic cavity, mainly in the lungs and mediastinal and tracheobronchial lymph nodes.

Although consistently present, the pulmonary changes varied between animals and affected all lung lobes; however, the caudal (inferior) lung lobe changes were generally more severe. One or more of the following pulmonary changes were observed: enlargement (failure to collapse); edema; mottled dark reddish-purple to black discoloration (consistent with severe pulmonary congestion, hemorrhage, and/or edema); and fibrinous pleuritis (a lesion seen more commonly on the pleural surface of the caudal [inferior] lung lobes). Fibrinous tags and adhesions loosely adhered to the thoracic wall and between the pleural surfaces of lung lobes, the diaphragm, and pericardial sac. Randomly scattered, well-circumscribed to coalescing, tannish-white, dome-shaped, firm to fluctuant necrotic foci ranging in size from 6 mm up to 2 cm in diameter effaced the pulmonary architecture of the inferior (caudal) lung lobes; however, similar lesions were randomly distributed in other lobes (Figure 5).

The most commonly affected lymph nodes were the mediastinal and tracheobronchial lymph nodes. However, similar findings were present in the mandibular, axillary, inguinal, and mesenteric lymph nodes. Enlargement (lymphadenopathy) with edema and reddish discoloration (suggestive of hemorrhage/congestion) were the most common nodal change.

Splenic changes were also common but variable between animals. The most noteworthy macroscopic lesion consisted of few to many (too numerous to count), up to 4 mm in diameter, tannish-white, flattened to slightly raised foci randomly dispersed throughout the parenchyma and capsular surface. Though common, the necrotizing foci were not always present. In some

cases, a normal sized to moderately enlarged (splenomegaly), dark-reddish brown turgid spleen (suggestive of diffuse congestion and/or hemorrhage) was the sole splenic finding.

Within the abdominal cavity, a mildly enlarged, dark reddish brown, congested liver (hepatomegaly) with an accentuated lobular pattern was observed in half of the animals. Occasionally, randomly distributed, 1-2 mm tannish-white necrotizing foci were seen on the hepatic surface; similar lesions were seen on the renal capsular surface of one animal. Blood tinged abdominal fluid was an infrequent finding. Non-specific congestion was observed in many tissues possibly attributed to cardiovascular collapse following euthanasia. In this study, however, congestion and/or hemorrhage specifically in the adrenal gland, pancreas, the urinary bladder mucosa, and throughout the gastrointestinal tract was likely due to *F. tularensis* infection.

Although there was variation, almost all animals had noteworthy histopathologic lesions specifically in the lung, lymph nodes, spleen, and bone marrow, which correlated well with the gross postmortem changes. Lesions were similar but varied in severity consisting of necrotizing and suppurative bronchopneumonia (associated with larger conducting airways and arterioles) to randomly distributed, vague to discrete inflammatory nodules (consistent with chronic abscesses and pyogranulomatous pneumonia). The latter was more common especially as the disease progressed. Random and coalescing necrotizing lymphadenitis, splenitis, and myelitis in multiple lymph nodes, spleen, and bone marrow, respectively, were consistently present. Immunolabeled intra- or extracellular bacteria, bacterial fragments, and/or antigen were most commonly seen in foci of necrosis.

Discussion

To evaluate medical countermeasures for inhalational tularemia, it is essential the proposed animal model utilizes infection via the aerosol route since disease progression varies

depending on the route of infection. To characterize the progression of inhalational tularemia in cynomolgus macaques, groups of cynomolgus macaques were exposed to target doses of 50, 500 or 5000 CFU of aerosolized *F. tularensis.* Survival was dose dependent with target doses of 500 CFU (134 to 749 CFU range) and 5000 CFU (1177 to 5860 CFU range) causing 100% lethality by Days 17 and 8, respectively. Target doses of 50 CFU (10 to 110 CFU range) resulted in 20% survival.

Tularemic disease manifestation is dependent on the route of infection, the dose, virulence of the strain, and host immune response [1, 20]. After exposure, *F. tularensis* multiplies at the initial site of infection prior to spreading to the regional lymph nodes, liver and spleen[11, 21]. After an average incubation period of 3-5 days there is an onset of symptoms including fever, chills, cough, headache, general malaise and in some cases diarrhea[20]. In this study, cynomolgus macaques displayed early signs of disease caused by exposure to aerosolized *F. tularensis* including anorexia, changes in behavior, and fever around Day 3. Increases in body temperature were observed as early as 2.8 days after the challenge for the high dose group and as late as 4.2 days after the challenge for the low dose group. Observed changes in behavior included decreased grooming, general decrease in activity or subdued behavior, less interaction with technical staff and isolated positioning in the cage starting Day 2. All animals had changes in behavior by Day 5. Loose stool was observed in some of the animals. Cough was observed in most of them.

Hematology and clinical chemistry parameters in humans infected with *F. tularensis* have not shown any consistent remarkable findings. A review of 88 cases of tularemia from 1949 through 1979 reported increased white blood cell counts ranging from 5,000 to 22,000 cells/mm^3 (median 10,400 cells/mm^3) upon hospital admission[22]. An additional review of over 300 of cases reported that 50% presented with WBC counts between 3,000 and 24,000 cells/mm^3 however the other half showed marked increases in leukocytes as great as 56,000 cells/mm^3 [22]. Similarly, in this study, there was a clear increase in WBC by Day 3 followed by a sharp decrease between Days 4 and 6 for all animals, however no group fell outside of the normal range such that it reached statistical significance. Increases in liver enzymes AST, ALT, and ALKP, as seen in this study, have been previously reported in human tularemia cases where of 58 patients tested, 58% had elevations in at least one of these three enzymes [22]. After initial

infection, *F. tularensis* multiplies in the regional lymph nodes and following dissemination it causes necrosis in organs such as the liver [33], which correlates with the observed increase in these enzymes.

Based on the macroscopic and microscopic findings of animals in this study, the lung, lymph nodes (particularly the mediastinal and tracheobronchial lymph nodes), spleen, liver, and bone marrow were the most severely affected tissues during *F. tularensis* infection regardless of challenge dose. Although varying in severity, multifocal and coalescing, necrotizing and pyogranulomatous pneumonia and abscessation with (or without) extensive edema, fibrinous pleuritis, and pleural fibrosis were consistent findings in almost all animals and correlated with the intra-thoracic histopathologic changes. Additionally, necrotizing mediastinal lymphadenitis, splenitis myelitis, and hepatitis were consistently observed regardless of the inhaled *F. tularensis* dose. The random focal necrotizing lesions in the liver were easily recognized but generally no greater than 100 µm in diameter unlike the larger coalescing lesions seen in the lung and spleen.

The severity of clinical signs and time-to-death following exposure were challenge dose-dependent (i.e. high dose-challenged animals generally met euthanasia criteria earlier than animals challenged with lower doses). However, similar macroscopic and microscopic lesions (especially in the target organs) were observed in both middle and low dose group animals. Although large inhaled doses may cause an animal to succumb to infection earlier, infection following exposure to a lower dose may result in *F. tularensis* dissemination and replication to higher numbers in tissues other than the lungs.

Here we demonstrated aerosolized *F. tularensis* infection in cynomolgus macaques causes similar disease progression and pathogenesis as compared to respiratory tularemia in humans. Therefore the cynomolgus macaque model of pneumonic tularemia is an appropriate animal model for testing medical countermeasures for treatment of tularemia.

Acknowledgments

We thank the personnel in the Aerosol Services Branch of the Center for Aerobiological Sciences for conducting the aerosol sprays of animals, the personnel of the Veterinary Medicine Division for the care and handling of the animals and the Clinical Lab personnel for performing hematology and chemistry tests in these studies. Special thanks to Pathology Division's Stephen Akers, Neil Davis, Gale Kreitz, and Chris Mech for providing necropsy, histochemical, and immunohistochemical support. Furthermore, we gratefully acknowledge Diana Fisher and Sarah Norris for their assistance with statistics, and Ondraya Frick for her assistance with the report. We also thank Judy Hewitt (NIAID) for excellent discussion and guidance during this study and Tina Guina (NIAID) for reviewing the report and data critically.

This study was supported by an interagency agreement between Office of Biodefense, Research Resources and Translational Research (OBRRTR)/National Institute of Allergy and Infectious Diseases (NIAID) and USAMRIID.

Disclaimer: Opinions, interpretations, conclusions, and recommendations are those of the authors and are not necessarily endorsed by the US Army or the Department of Defense.

References

1. Nigrovic LE, Wingerter SL. Tularemia. Infectious disease clinics of North America. 2008;22(3):489-504, ix. doi: 10.1016/j.idc.2008.03.004. PubMed PMID: 18755386.

2. Dennis DT, Inglesby TV, Henderson DA, Bartlett JG, Ascher MS, Eitzen E, et al. Tularemia as a biological weapon: medical and public health management. Jama. 2001;285(21):2763-73. PubMed PMID: 11386933.

3. Hepburn MJ, Friedlander AM, Dembek ZF. Tularemia. In: Lenhart MK, editor. Medical Aspects of Biological Warfare. Washington, D.C.: Borden Institute; 2007. p. 167-84.

4. Helvaci S, Gedikoglu S, Akalin H, Oral HB. Tularemia in Bursa, Turkey: 205 cases in ten years. European journal of epidemiology. 2000;16(3):271-6. PubMed PMID: 10870943.

5. Komitova R, Nenova R, Padeshki P, Ivanov I, Popov V, Petrov P. Tularemia in bulgaria 2003-2004. Journal of infection in developing countries. 2010;4(11):689-94. PubMed PMID: 21252445.

6. Reintjes R, Dedushaj I, Gjini A, Jorgensen TR, Cotter B, Lieftucht A, et al. Tularemia outbreak investigation in Kosovo: case control and environmental studies. Emerging infectious diseases. 2002;8(1):69-73. PubMed PMID: 11749751; PubMed Central PMCID: PMC2730257.

7. Tularemia WHOWGo.

8. Steiner DJ, Furuya Y, Metzger DW. Host-pathogen interactions and immune evasion strategies in Francisella tularensis pathogenicity. Infection and drug resistance. 2014;7:239-51. doi: 10.2147/IDR.S53700. PubMed PMID: 25258544; PubMed Central PMCID: PMC4173753.

9. Alibek K. Biohazard. New York, New York: Random House, Inc.; 1999.

10. Kortepeter MG, Parker GW. Potential biological weapons threats. Emerging infectious diseases. 1999;5(4):523-7. doi: 10.3201/eid0504.990411. PubMed PMID: 10458957; PubMed Central PMCID: PMC2627749.

11. Oyston PC, Sjostedt A, Titball RW. Tularaemia: bioterrorism defence renews interest in Francisella tularensis. Nature reviews Microbiology. 2004;2(12):967-78. doi: 10.1038/nrmicro1045. PubMed PMID: 15550942.

12. Thomas LD, Schaffner W. Tularemia pneumonia. Infectious disease clinics of North America. 2010;24(1):43-55. doi: 10.1016/j.idc.2009.10.012. PubMed PMID: 20171544.

13. Feldman KA, Enscore RE, Lathrop SL, Matyas BT, McGuill M, Schriefer ME, et al. An outbreak of primary pneumonic tularemia on Martha's Vineyard. The New England journal of medicine. 2001;345(22):1601-6. doi: 10.1056/NEJMoa011374. PubMed PMID: 11757506.

14. Teutsch SM, Martone WJ, Brink EW, Potter ME, Eliot G, Hoxsie R, et al. Pneumonic tularemia on Martha's Vineyard. The New England journal of medicine. 1979;301(15):826-8. doi: 10.1056/NEJM197910113011507. PubMed PMID: 481515.

15. Lyons RCW, Terry H. Animal models of *Francisellla tularensis* infection. In: Abu Kwaik Y, Nano F, Sjostedt A, Titball RW, editors. *Francisella tularensis*: biology, pathogenicity, epidemiology, and biodefense. New York, NY: The New York Academy of Sciences; 2007.

16. Glynn AR, Alves DA, Frick O, Erwin-Cohen R, Porter A, Norris S, et al. Comparison of experimental respiratory tularemia in three nonhuman primate species. Comparative immunology, microbiology and infectious diseases. 2015;39:13-24. doi: 10.1016/j.cimid.2015.01.003. PubMed PMID: 25766142; PubMed Central PMCID: PMC4397973.

17. Dabisch PA, Kline J, Lewis C, Yeager J, Pitt ML. Characterization of a head-only aerosol exposure system for nonhuman primates. Inhalation toxicology. 2010;22(3):224-33. doi: 10.3109/08958370903191023. PubMed PMID: 20063997.

18. Christensen DR, Hartman LJ, Loveless BM, Frye MS, Shipley MA, Bridge DL, et al. Detection of biological threat agents by real-time PCR: comparison of assay performance on the R.A.P.I.D., the LightCycler, and the Smart Cycler platforms. Clinical chemistry. 2006;52(1):141-5. doi: 10.1373/clinchem.2005.052522. PubMed PMID: 16391330.

19. Prophet EB, Mills B, Arrington JB, Sobin LH. Laboratory Methods for Histotechnology. Washington, D.C.: Armed Forces Institute of Pathology; 1992.

20. Dienst FT, Jr. Tularemia: a perusal of three hundred thirty-nine cases. J La State Med Soc. 1963;115:114-27. PubMed PMID: 14027775.

21. Santic M, Molmeret M, Klose KE, Abu Kwaik Y. Francisella tularensis travels a novel, twisted road within macrophages. Trends Microbiol. 2006;14(1):37-44. doi: 10.1016/j.tim.2005.11.008. PubMed PMID: 16356719.

22. Evans ME. Francisella tularensis. Infect Control. 1985;6(9):381-3. PubMed PMID: 3850862.

Table 1: Comparison of Animal Survival between Groups

Group	Average Inhaled Dose (CFU)	Days to Death*		Survivals/Total	Average Weight Loss (%)
		Mean	Std. Dev.		
50 CFU	49	11.9	4.5	2/10	2.4
500 CFU	506	8.4	3.4	0/10	8.7
5000 CFU	4040	7.1	0.9	0/10	8.3

***** Non-survivors

Table 2: Survival Statistics (p-values)

Group Comparison	% Survival (p-values)	Time-to-Death (Days) (p-values)	Survival Curve (p-values)
50 CFU vs. 500 CFU	1.0000	0.2117	**0.0324**
50 CFU vs. 5000 CFU	1.0000	0.0630	**0.0036**
500 CFU vs. 5000 CFU	1.0000	0.2891	0.4228

Figure 1: Survival of cynomolgus macaques exposed to increasing doses of aerosolized *F. tularensis*. Group sizes were 50 CFU (n=10), 500 CFU (n=9), and 5000 CFU (n=9).

Figure 2: Body Temperature for three groups of NHPs exposed to increasing doses of *F. tularensis*. Fever was defined as a body temperature two standard deviations above the baseline.

Figure 3: A) White blood counts (WBC), **B)** Neutrophils (NEU), **C)** Lymphocytes (LYM) **and D)** Platelets (PLT) of cynomolgus macaques exposed to *F. tularensis*. EDTA whole blood was analyzed on the Abbott Cell-Dyn 3700 hematology analyzer.

Figure 4: Liver function parameters **(A-E)** and Lactate Dehydrogenase (LDH) **(F)** was tested for cynomolgus macaques exposed to different doses of *F. tularensis*. **A)** Total protein (Total Bili),

B) Albumin, **C)** Aspartate Transaminase (AST), **D)** Alanine Transaminase (ALT), **E)** Alkaline Phosphatase (ALKP). Analysis of clinical chemistry parameters was performed using an Ortho-Clinical Diagnostics Vitros 250 chemistry analyzer.

Figure 5: Quantitative bacteremia in **A)** whole blood and **B)** tissues was determined using real-time PCR of duplicate samples. Average result using data from both runs are reported.

Figure 6: A) Normal lung from a non-challenged cynomolgus macaque. **B)** Representative of low dose lung (31 CFU); hemorrhagic, edematous, and non-collapsing lung with extensive fibrin deposition on the pleural surface (fibrinous pleuritis). **C)** Representative of high dose lung (5140 CFU); multiple, raised necrotizing, and/or pyogranulomatous foci on all lung lobes. **D)** High dose lung (5140 CFU); closer view of Figure 6D; not the hemorrhage and congestion between foci with fibrin strands between lobes (arrow).

Figure 1

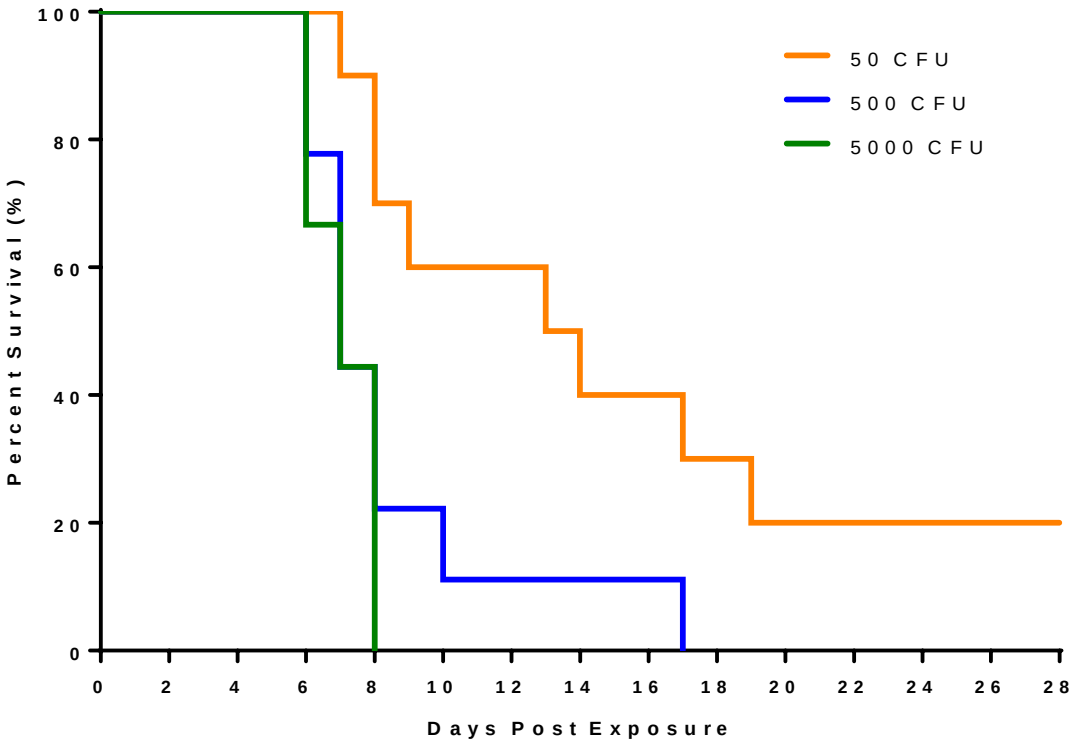
100
80
60
40
20
0
Percent Survival (%)
0
2
4
6
8
10
12
14
16
18
20
22
24
26
28
Days Post Exposure
50 CFU
500 CFU
5000 CFU

Figure 2

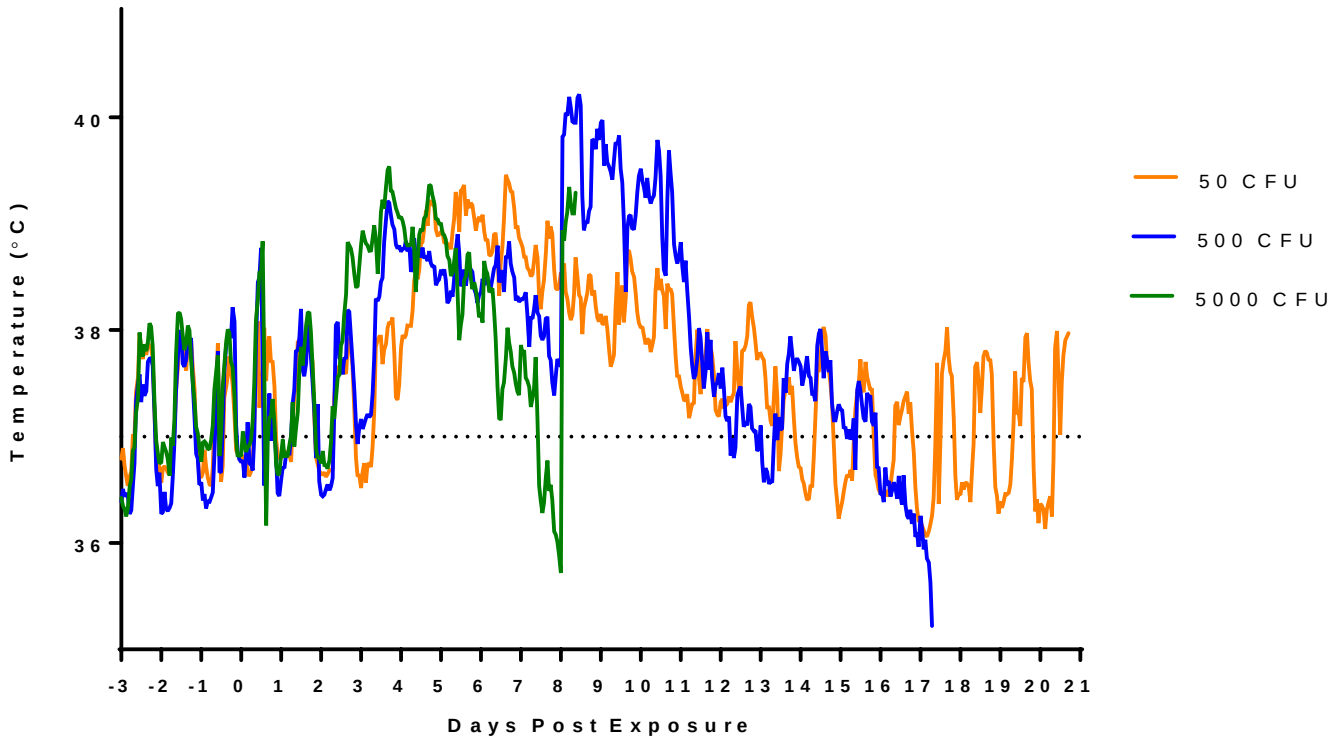
Temperature (°C)
40
38
36
-3 -2 -1 0 1 2 3 4 5 6 7 8 9 10 11 12 13 14 15 16 17 18 19 20 21
Days Post Exposure
50 CFU
500 CFU
5000 CFU

Figure 3

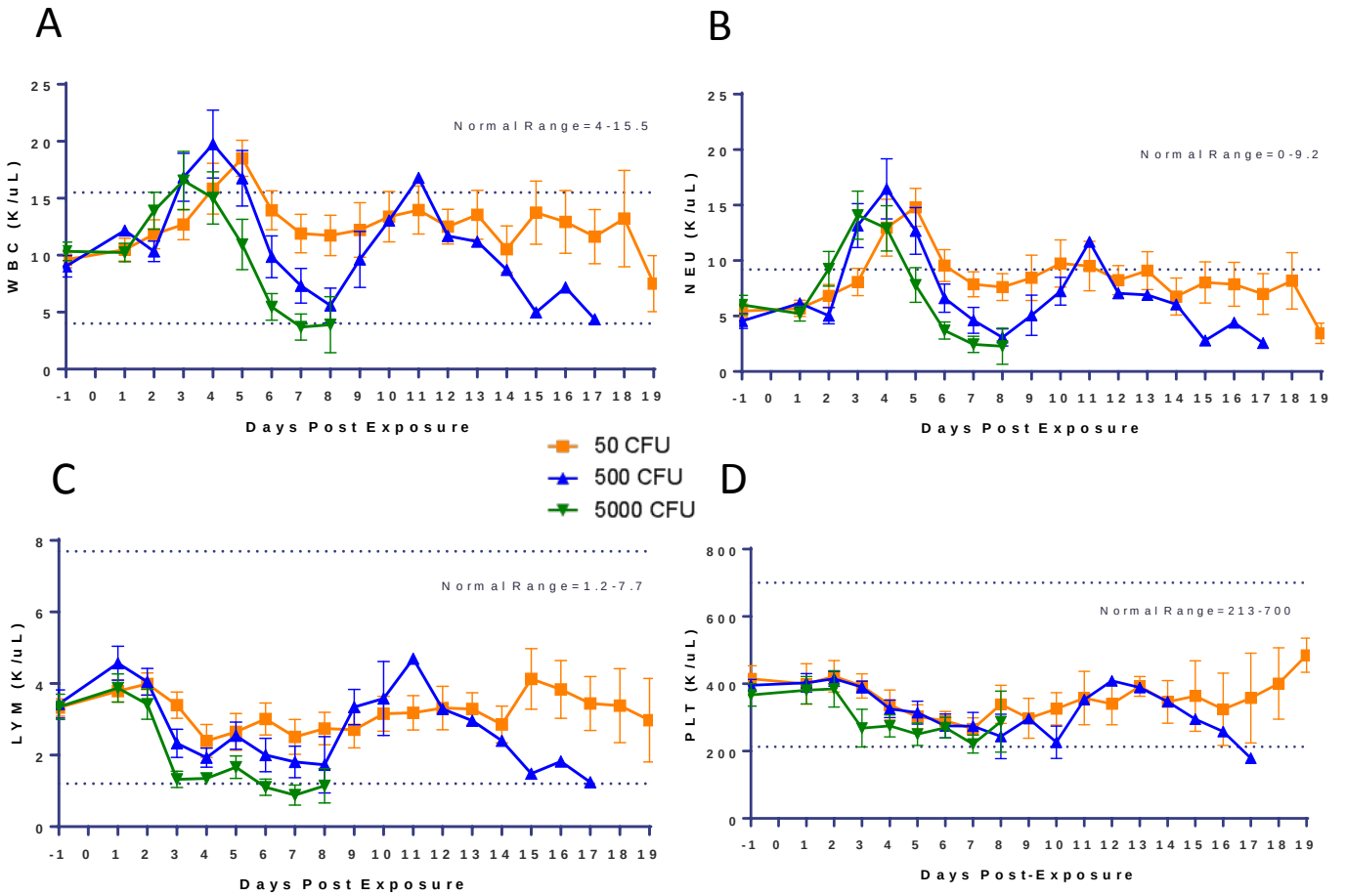
A
B
C
D
WBC (K/uL)
NEU (K/uL)
LYM (K/uL)
PLT (K/uL)
Normal Range=4-15.5
Normal Range=0-9.2
Normal Range=1.2-7.7
Normal Range=213-700
Days Post Exposure
Days Post-Exposure
50 CFU
500 CFU
5000 CFU

Figure 4

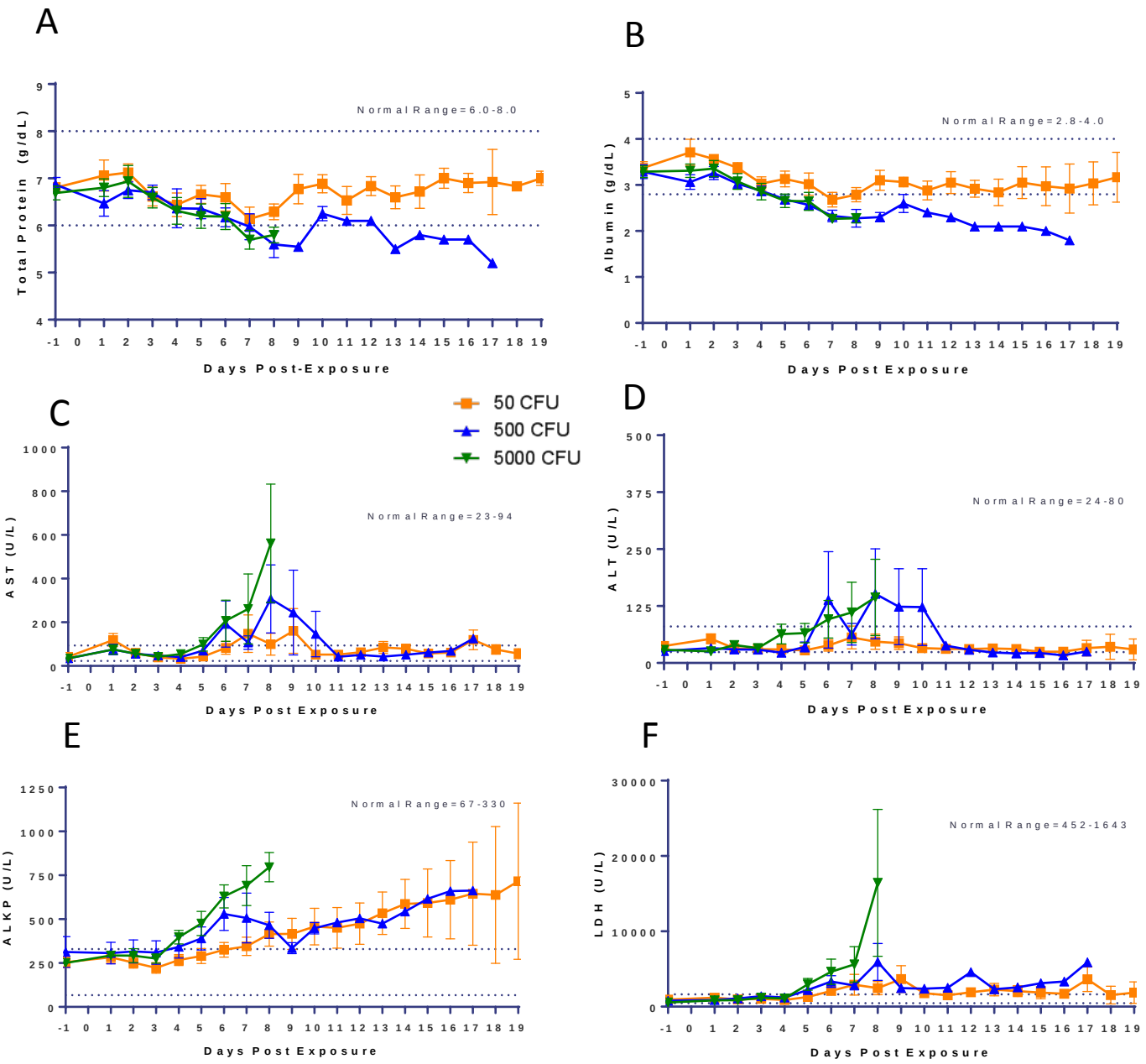
A
Normal Range=6.0-8.0
Total Protein (g/dL)
Days Post-Exposure
B
Normal Range=2.8-4.0
Albumin (g/dL)
Days Post Exposure
C
50 CFU
500 CFU
5000 CFU
Normal Range=23-94
AST (U/L)
Days Post Exposure
D
Normal Range=24-80
ALT (U/L)
Days Post Exposure
E
Normal Range=67-330
ALKP (U/L)
Days Post Exposure
F
Normal Range=452-1643
LDH (U/L)
Days Post Exposure

Figure 5

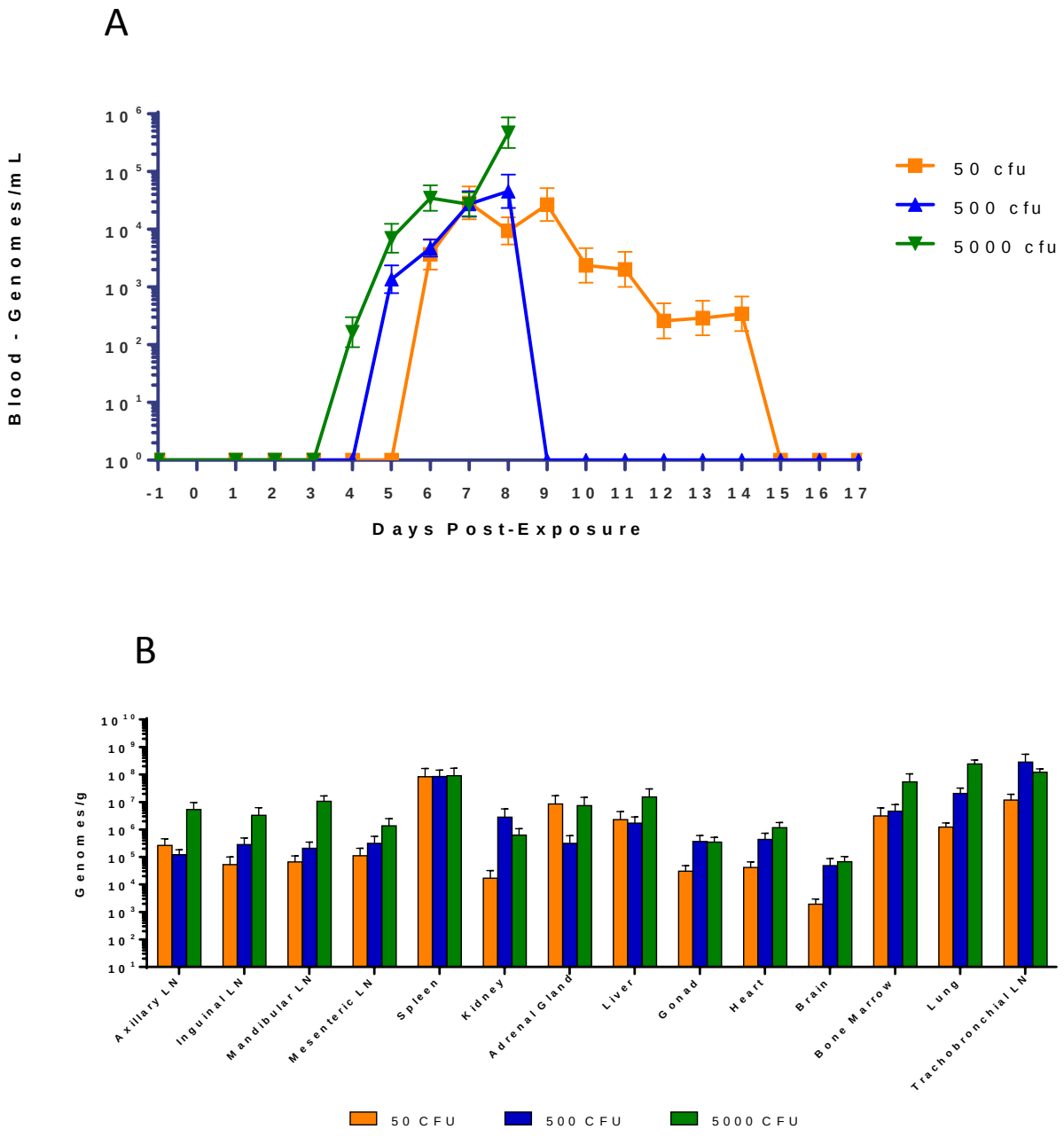
A
Blood - Genomes/mL
10^6
10^5
10^4
10^3
10^2
10^1
10^0
-1 0 1 2 3 4 5 6 7 8 9 10 11 12 13 14 15 16 17
Days Post-Exposure
50 cfu
500 cfu
5000 cfu
B
Genomes/g
10^10
10^9
10^8
10^7
10^6
10^5
10^4
10^3
10^2
10^1
Axillary LN
Inguinal LN
Mandibular LN
Mesenteric LN
Spleen
Kidney
Adrenal Gland
Liver
Gonad
Heart
Brain
Bone Marrow
Lung
Trachobronchial LN
50 CFU
500 CFU
5000 CFU

Figure 6